Smart Grid and Renewable Energy, 2023, 14, 15-29
https://www.scirp.org/journal/sgre
ISSN Online: 2151-4844
ISSN Print: 2151-481X

Microgrid Optimal Scheduling

Salem Al-Agtash[1,2*], Mohamad Al Hashem[2]

[1]Department of Computer Science and Engineering, Santa Clara University, Santa Clara, CA, USA
[2]Department of Computer Engineering, German Jordanian University, Amman, Jordan
Email: *salagtash@scu.edu

How to cite this paper: Al-Agtash, S. and Al Hashem, M. (2023) Microgrid Optimal Scheduling. *Smart Grid and Renewable Energy*, **14**, 15-29.
https://doi.org/10.4236/sgre.2023.142002

Received: January 30, 2023
Accepted: February 21, 2023
Published: February 24, 2023

Abstract

This paper presents the optimal scheduling of renewable resources using interior point optimization for grid-connected and islanded microgrids (MG) that operate with no energy storage systems. The German Jordanian University (GJU) microgrid system is used for illustration. We present analyses for islanded and grid-connected MG with no storage. The results show a feasible islanded MG with a substantial operational cost reduction. We obtain an average of $1 k daily cost savings when operating an islanded compared to a grid-connected MG with capped grid energy prices. This cost saving is 10 times higher when considering varying grid energy prices during the day. Although the PV power is intermittent during the day, the MG continues to operate with a voltage variation that does not 10%. The results imply that MGs of GJU similar topology can optimally and safely operate with no energy storage requirements but considerable renewable generation capacity.

Keywords

Microgrid, Renewable Energy, Optimal Scheduling, Power Flow

1. Introduction

Microgrids (MGs) are small-size controllable power systems that use renewable generation resources, such as solar, wind, and biomass. They are characterized as resilient small-scale power systems that can withstand failures [1] [2] [3]. Deploying MGs has become increasingly feasible, reliable, and cost-effective with high penetration of renewable energy resources. MGs generally complement utility grids and operate as grid-connected or islanded electric power systems. A grid-connected MG exchanges power with the utility grid. An Islanded MG operates as a stand-alone small-size power grid.

The power of renewable resources is, by nature, intermittent. This impacts the stability of MGs if not properly controlled to maintain the generation-load balance in real-time. The availability of energy storage or connection to a utility grid provides potential sources of microgrid stabilization. Energy storage has a high initial cost, and its lifetime is short. Furthermore, MGs in distant areas are not connected to the power grid. Under these scenarios, optimally scheduling MG resources while maintaining a reliable microgrid with a consistent generation-load balance has been a challenging research problem.

However, the current research in MG resource scheduling is generalized in the context of the MG topology and elements. [4] presents a two-stage adaptive robust optimization model for minimizing operational costs while increasing resiliency against high-impact and low-probability events. In [5] [6] [7], stochastic programming methods were used to address the uncertainty of power demand and renewable energy resources. A novel binary backtracking search algorithm has been introduced to control switching local power generation resources [8]. Scheduling based on shaping the power demand curve was presented in [9] [10] [11] to devise optimal scheduling of grid-connected MG, mainly using multi-dimensional competitive and mixed integer non-linear programming algorithms. Experimental analysis on optimizing the operation of a real grid-connected MG has been presented in [12]. [13] presents an analytical target cascading method to construct a stakeholder-parallelizing distributed robust adaptive optimization for multi-microgrids. [14] investigates the feasibility of scheduling distributed energy resources while considering voltage and frequency constraints. [15] shows scheduling MG resources in grid-connected or islanded modes with energy storage to achieve generation-load balance.

This research is motivated by the need to study resource scheduling of MGs with no energy storage since energy storage requires high initial investment costs and their lifetime is short. We use the MG of the German Jordanian University as a case study of this research. Like GJU, many MGs operate without energy storage. We present optimal scheduling of MG resources using interior point optimization for both islanded and grid-connected operations. In an islanded operation, Diesel Generation (DG) is used to complement the renewable generation that is intermittent in nature and to provide MG stability. The results show a feasible islanded MG with a substantial operational cost reduction while guaranteeing power availability to balance the power load in real time.

The remainder of this paper is organized as follows: Section 2 presents a microgrid system. The problem formulation and optimal scheduling are presented in Sections 3 and 4. Section 5 provides details of the microgrid application of GJU. Section 6 presents the testing results of MG optimal scheduling. Finally, the paper is concluded in Section 7.

2. Microgrid System

Microgrids generally comprise several renewable generation resources and loads and are managed and operated in real-time either in a grid-connected or islanded mode.

2.1. Generation

Renewable generation comprises solar and wind resources generally complemented by on-site diesel generators, energy storage batteries, and interconnection to the main power grid. Storage batteries typically have a short lifetime and are expensive to install.

Solar power

Solar power is produced by a large array of photovoltaic cells, formally defined as [16]:

$$P_{pv} = \eta AG\left(1-\alpha\left(T-25\right)\right) \tag{1}$$

where G, T, A, η, and α denote solar radiation, ambient temperature, area of panels, system efficiency, and power degradation, respectively. The output power of the photovoltaic array at substation i is formally defined as:

$$P_{pv}\left(t\right) = \sum_{i=1}^{N_{pv}} P_{pvi}\left(t\right) \tag{2}$$

where N_{pv} represents the number of substations connecting photovoltaic arrays.

Diesel Generators

Since the output power of solar and wind is intermittent and non-controllable, it is necessary to have storage and controllable generation in the microgrid that can replace power shortage and maintain constant local power. The output power of N diesel generators is formally defined as:

$$P_G\left(t\right) = \sum_{i=1}^{N} P_{Gi}\left(t\right) \tag{3}$$

where $P_{Gi}\left(t\right)$ denotes the output power of the ith diesel generator at time t. The cost of power is defined as [17]:

$$C_i\left(P_{Gi}\left(t\right)\right) = A\left(F\left(P_{Gi}\left(t\right)\right)+C_i^{fixed}\right)\Delta t \tag{4}$$

where C_i, A, F, and Δt denote the cost ($), price of diesel ($/Liter), variable cost, and time interval, respectively.

2.2. Utility Power

In a grid-connected mode, the operational cost also includes the cost of power absorbed from the utility grid. The cost depends on the market selling price of power $P_{Gr}\left(t\right)$ absorbed from or injected to the utility grid at time t, defined as:

$$C_{Gr}\left(P_{Gr}\left(t\right)\right) = \rho\left(t\right)P_{Gr}\left(t\right) \tag{5}$$

where $\rho\left(t\right)$ denotes the energy price at utility grid ($/kWh) at time t. A negative value represents energy sold from MG to the utility grid.

2.3. Load Profile

MG load profiles are generally time-varying and are shaped by the type of load. In a university campus, the load profile is given by the power demand $P_D\left(t\right)$ at time t, defined as:

$$P_D\left(t\right) = \begin{cases} A & t_1 \le t < t_2 \\ B\sin\left(\omega\left(t\right)-\phi\right)+A & t_2 \le t < t_3 \\ A & t_3 \le t < t_4 \end{cases} \tag{6}$$

where A and B are constants and can be calculated using the curve fitting of the historical power demand data. Furthermore, w and ϕ denote the angular frequency and the phase shift of power demand, respectively.

3. Problem Formulation

We consider GJU microgrid architecture for the problem formulation of scheduling. The high operational cost of MG is mainly given by the cost of power produced by the diesel generators and the cost of power absorbed or injected into the utility grid. The objective function $\pi : G \to R$ is, therefore, formally defined as:

$$\pi\left(P_{Gr}, P_{Gi}\right) = \sum_{t=0}^{24} C_{Gr}\left(P_{Gr}\left(t\right)\right) + \sum_{i=1}^{N} C_i\left(P_{Gi}\left(t\right)\right) \tag{7}$$

where:

- $C_{Gr}\left(P_{Gr}\left(t\right)\right)$ and $C_i\left(P_{Gi}\left(t\right)\right)$ denote the cost of power that comes from utility grid at time t and the cost of power produced by the i^{th} diesel generator at time t.
- P_{Gr} and P_{Gi} denote vectors of 24 elements representing day-ahead schedules in the set G that maps to the set of real numbers R.

The MG operates under the following various constraints:

1) Generation – Load balance

$$\sum P_G\left(t\right) = P_D\left(t\right) - P_{RES}\left(t\right) - P_{Gr}\left(t\right) - P_{Loss}\left(t\right) \tag{8}$$

where:

$P_{RES}\left(t\right)$: Output power from different available renewable energy sources.

$P_{Loss}\left(t\right)$: Losses in the distribution lines.

$P_D\left(t\right)$: Power demand

2) Limits of the i^{th} diesel generators output power

$$P_{Gi}^{\min} \le P_{Gi}\left(t\right) \le P_{Gi}^{\max} \tag{9}$$

where:

$P_{Gi}^{\min}$: Minimum output power of the i^{th} diesel generator.

$P_{Gi}^{\max}$: Maximum output power of the i^{th} diesel generator.

3) Local power availability level (Lav) and utility grid power fraction (fav), defined as:

$$Lav\left(t\right) = \left(1 - fav\left(t\right)\right) * 100\% \tag{10}$$

$$fav\left(t\right) = \frac{P_{Gr}\left(t\right)}{P_D\left(t\right)} \tag{11}$$

where Lav is in the range:

$$Lav^{\min} \le Lav\left(t\right) \le Lav^{\max} \tag{12}$$

Let the equality and inequality constraints (8) - (12) be denoted by a real-valued vector $h\left(P_{Gr}, P_{Gi}\right)$, the scheduling problem is then formally defined with an objective function π as:

$$\min_{P_{Gr},P_{Gi}\in R} \pi\left(P_{Gr},P_{Gi}\right) \text{ subject to: } h\left(P_{Gr},P_{Gi}\right)\le 0 \quad (13)$$

We seek to find the optimal schedules of the day-ahead P_{Gr} and P_{Gi}, that minimize the operational costs of MG while satisfying the various constraints. This problem is a non-convex nonlinear programming problem, and a closed-form solution does not exist.

4. Optimal Scheduling

The optimization in microgrid scheduling has been presented in several articles, including [18] [19] [20] [21]. We use the interior point method [22] for solving (13). In this method, the values of (Lav, fav, P_{Gr}, P_G, P_{Gi}) are updated iteratively. The values of (P_D, P_{RES}, $P_{Gi}^{\min}$, $P_{Gi}^{\max}$, $Lav^{\min}$, $Lav^{\max}$, C_i^{fixed}, K, and A are set constant and they represent MG operating constraints. Even though the power exchange between the MG and the utility grid is limited by (12), resiliency and reliability can still be enhanced. The following steps represent the interior point method:

1) Add slack variables to convert inequalities constraints into equalities.

2) Eliminate bounds on constraints by adding a barrier function into π.

3) Formulate Karush-Kuhn-Tucker (KKT) by taking the gradient of Lagrangian.

4) Linearize the equations by using Newton-Raphson method and solve iteratively.

5) Employ a line search using a merit function, trust regions, and filter methods.

Figure 1 gives a flow chart of the solution algorithm. An initial guess of power values $\left(P_{Gr},P_{Gi}\right)$ is made to compute the objective function π. The values are updated in the direction of the search for several iterations until convergence.

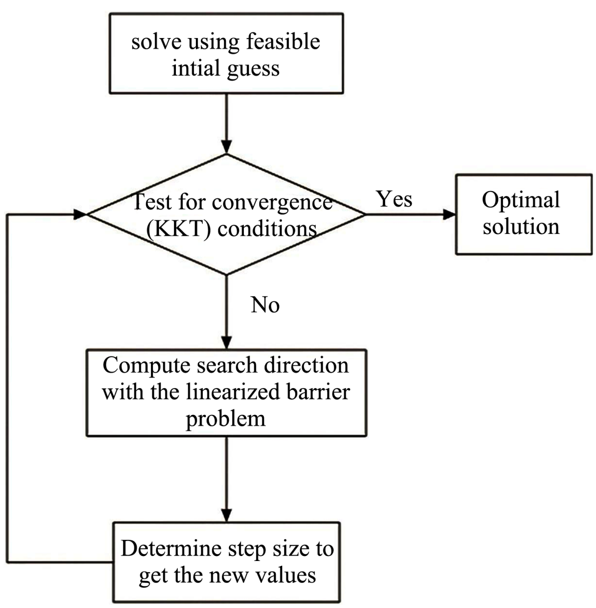

Figure 1. Flow chart of the solution.

We use APMonitor Optimization Suit (APM) with Interior Point OPTimizer (IPOPT) to implement the algorithm [23]. APM is optimization software for mixed-integer and algebraic differential equations. It can be used with MATLAB, Python, and a web interface.

5. Microgrid Application

The German Jordanian University (GJU) microgrid application is used for testing. It has been used for demonstration in the 3DMicrogrid project [24] and has been illustrated in MG-related research [25] [26] [27].

5.1. GJU Microgrid

GJU microgrid consists of PV generation interconnected with loads of sixteen buildings and a point of common coupling with the utility grid located in the main station south of campus. The main station contains two 33/11kV transformers. Each of these transformers feeds a group of three 11/0.4kV transformers around the campus feeding the buildings. These two groups of transformers are connected in a ring configuration via a circuit breaker between transformers 1 and 6 to support the reliability and flexibility of the microgrid. **Figure 2** shows a detailed snippet of the GJU single-line diagram with one substation connecting to a 0.45 MWP PV station, 1.6 MW load, 0.4 MVAR capacitor bank, and a 150 KVA backup Diesel Generator with 400/11kV transformer.

At GJU, six diesel generators are installed in buildings A to F. They are used to accommodate the intermittence of PV resources. The ratings in kVA for the transformers (T1, T3, T5, and T6) and (T2 and T4) are 1000 and 1500, respectively. The Power Factor is 0.95 and is driven by six capacitor banks with a total value of 1200 kVar in buildings: A, B, C, H, and M. A single controllable point of interconnection to the main grid exists with a circuit breaker on for a grid-connected mode and off for an isolated mode. The substation at the interconnection has 33/11kV transformer, which interconnects to the main grid for a two-way power flow. The transmission lines interconnect generation resources and building substations with 11/.4kV bus transformers.

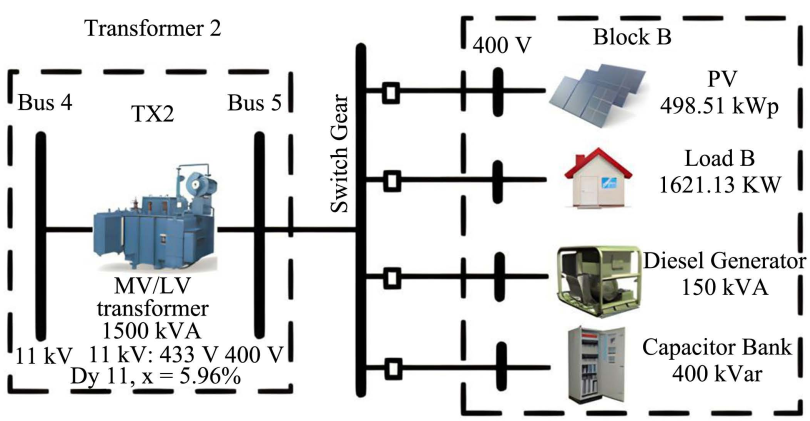

Figure 2. Single-line diagram for one substation.

5.2. Load Profile

The loads at GJU are categorized in buildings A, B, C, D, E, and F as essential, nonessential, and air conditioning. These loads are remotely controllable via controllable circuit breakers. Figure 3 shows a typical load profile for a Winter and a Summer Day, where peak loads occur during working hours 8:00-17:00 and is at 1.05 and 1.6 Mega Watt (MW), respectively.

Using (6), the curve-fitting values for this load profile are given as follow:

$$P_D(t) = \begin{cases} 195 & 0 \le t < 6 \\ 851.49\sin\left(15(t) - 82.5\right) + 195 & 6 \le t < 17.5 \\ 195 & 17.5 \le t < 24 \end{cases} \tag{14}$$

5.3. PV Generation

The PV power generation at GJU exists at Buildings B, D, E, and F, with a total capacity of 1.8 MW. The PV power generation for a Winter and a Summer Day is shown in Figure 4. The production patterns indicate the intermittent nature of PV with variations dependent on weather conditions.

6. Testing Results

In this section, the testing results are presented for the estimates of load and PV generation, operation cost analysis, and power flow and stability analysis for both grid-connected and islanded microgrids.

6.1. Load and PV Estimates

We use Equation (1) to compute the estimated PV power and Equation (6) to estimate the power demand a day ahead. Figure 5 and Figure 6 compare the

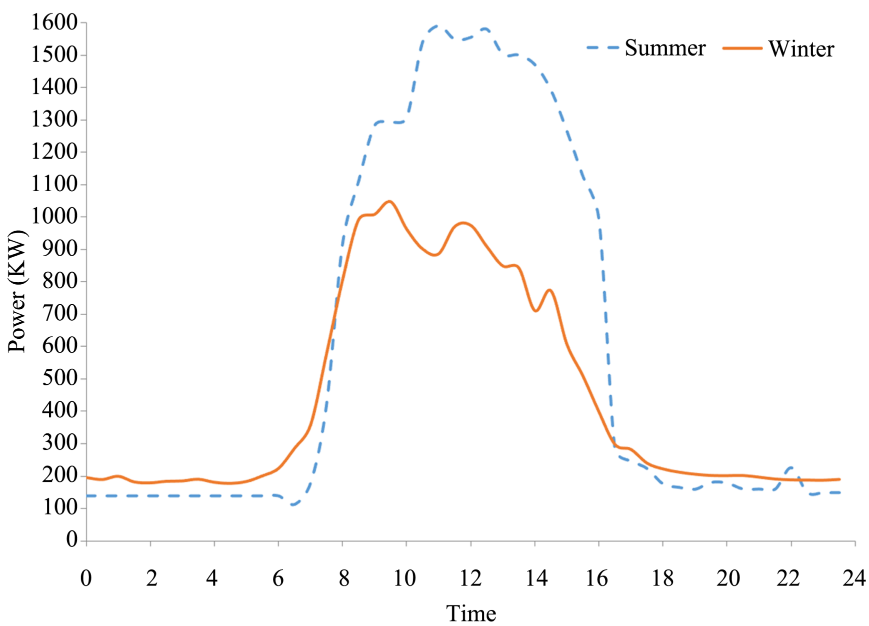

Figure 3. Load profile for summer and winter day.

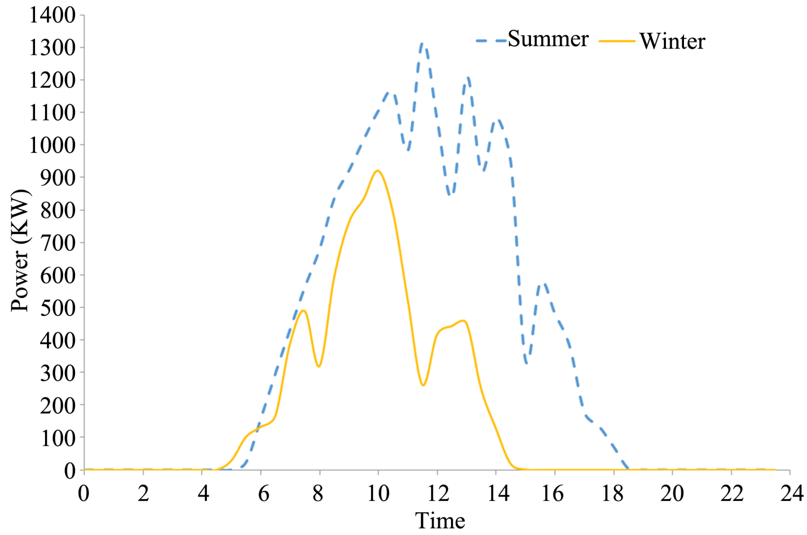

Figure 4. PV power generation for summer and winter day.

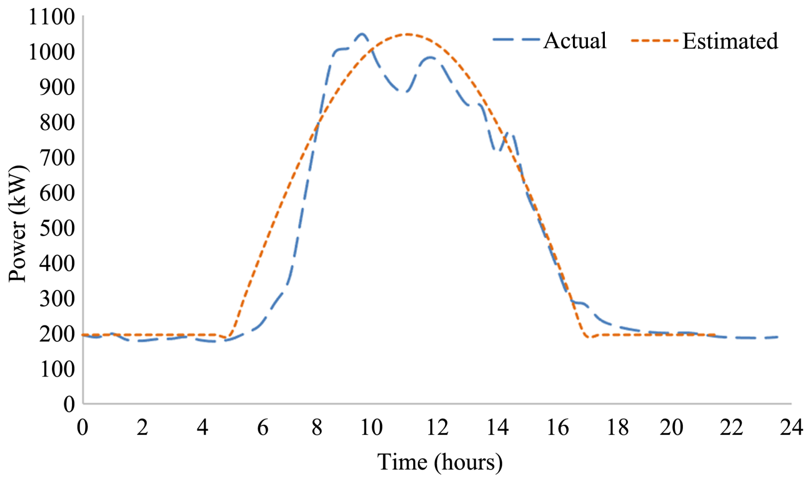

Figure 5. Actual and estimated power demand for 30/12/18.

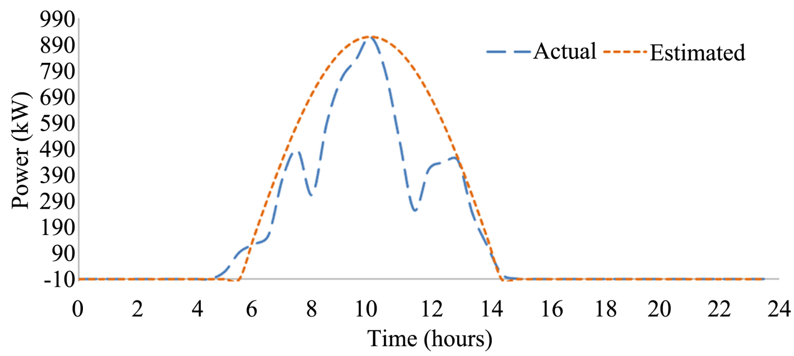

Figure 6. Actual and estimated PV power for 30/12/18.

actual and the estimated power demand and PV power generation for day 30/12/2018, respectively. The results indicate accurate power demand and generation estimates and represent an average variation of less than 10%.

6.2. Operational Cost Analysis

The operational cost analyses of GJU grid-connected MG are presented in this section. Since the output power of renewable energy is not controllable, and GJU has no energy storage, diesel generators are used to compensate for the power shortage in real time. For this purpose, one generator is turned on all the time. For the winter day analysis, only two generators: DG1 and DG2, were used. The rating of DG1 is 703 kVA, while DG2 is 350 kVA. We use the data sheets of the diesel generators to compute their operational costs. The parameters in (5) are then given as:

$$C_{DG1}(t) = A\left(0.0001 + 0.175 DG_1(t) + 19.62\right)\Delta t$$

$$C_{DG1}(t) = A\left(0.0001\left(DG_2(t)^2\right) + 0.2181 DG_2(t) + 5.6955\right)\Delta t$$

with $A = 0.68$ $/Liter.

We use two scenarios for the operational cost analysis. In scenario A, electricity prices remain constant. In scenario B, electricity prices vary.

Scenario A

In this scenario, the grid energy prices are constant and are set to 0.37 $/kWh. Power flow analyses are made on the winter day while the local power availability factor (*Lav*) is set to a range between 70% - 100%. The availability level varies at every time interval depending on the optimization results. Figure 7 shows the power demand, power flow of the utility grid, and power generation of PV and DGs. The results show that diesel generators replace utility grid power, and both PV and DG meet the GJU power demand. Therefore, the local power availability level during the day is 100%. This implies that the operating cost of diesel generators is much less than the utility grid. The operational cost of power (on the winter day) with a normal operation where power is supplied by the utility grid

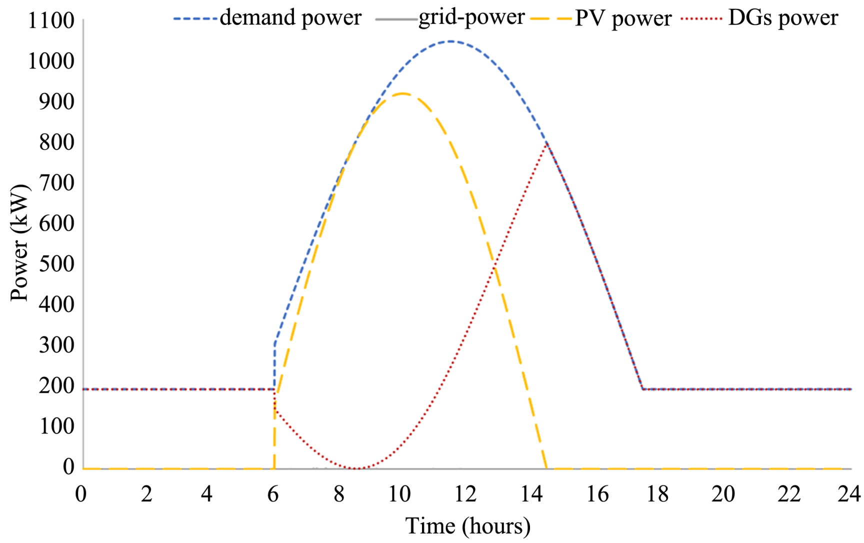

Figure 7. Power demand, grid power flow, PV power, and DGs power with constant grid energy prices – winter day and 70% - 100% local power availability.

and PV in a net metering configuration is $2176.9. In the islanded MG, the optimal operational cost gets reduced to $1086.5. In this case, the design can be set to sell power in case of excessive power generation.

Scenario B

In Scenario B, there are two load peaks: morning and evening. During these peaks, the cost of the grid power gets higher to shape the load. In this scenario, these peaks are assumed to be between the time intervals of 6:00-8:00 and 16:00-18:00. The price of the grid energy during these times is 0.37 $/kWh. During the other time intervals, the price is 0.17 $/kWh. The local power availability factor (Lav) is set to the 70% - 100% range. Figure 8 shows the power demand, power flow of the utility grid, and the power generation of PV and DGs. During off-peak, the power demand is met by PV, DG, and the utility grid. The operational cost of power (this winter day) with the normal operation when power is supplied by the utility grid and PV in a net metering configuration is $1157.84. In the islanded MG, the optimal operational cost gets reduced to $1082.64.

These results indicate that the utility grid's energy price drives the local power availability level. When prices get higher during peak hours, the MG raises the local power availability level to avoid buying energy from the utility grid at a high price. The power shortage is compensated solely by the DG. As a matter of fact, GJU operates an islanded MG as described in scenario A, which provides an average of $1k price reduction. We used scenario B as a hypothetical case to show the cost feasibility and sensitivity of MG scheduling. The results show that the variation of $Lav(t)$ is primarily driven by the energy prices of the utility grid. The total cost reduction in scenario B was lower because of the assumption of the grid's low energy prices during off-peak hours while meeting 70% of $Lav(t)$ minimum threshold value.

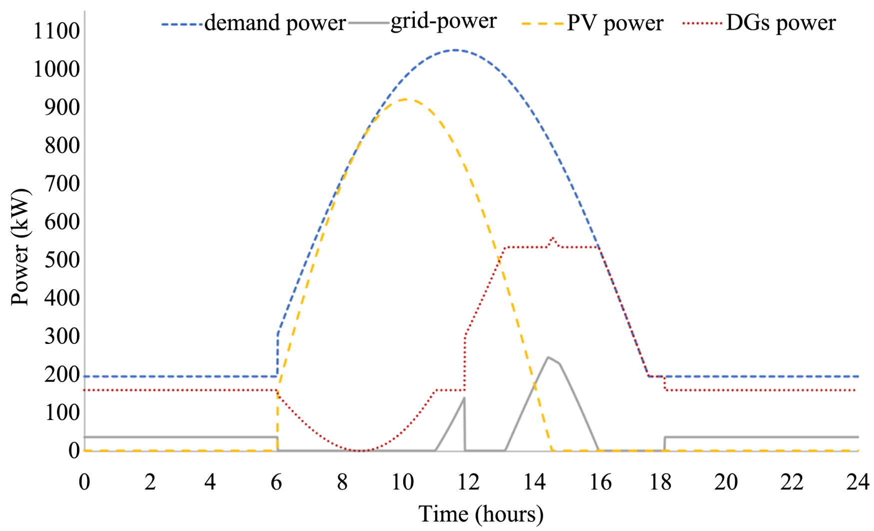

Figure 8. Power demand, grid power flow, pv power, and dgs power with varying grid energy prices – winter day and 70% - 100% local power availability.

6.3. Power Flow and Stability Analysis

We used the Phasor Simulation in MATLAB for symmetrical load profiles in a 1-minute resolution. The Power factor is set as 0.95 because of the availability of 1.2 MVAR capacitor banks distributed across the campus buildings. We used controlled current sources for each phase to represent the power demand and the PV system. The temperature and radiation readings in (1) were used to obtain the PV output power readings, where:

A: Area of panels (10462.38 m^2).

η: Overall efficiency of the system (13.5%).

α: Power degradation (0.45%).

We use scenario B to study the power flow and stability of GJU MG. This scenario provides a mix of generation resources that involve not only PV and DG power generation but also the power of the utility grid. Generally, a grid-connected MG does not encounter severe stability challenges. **Figure 9** shows the output power flow of PV, DG1, and DG2. Since DG1 was turned on at 11:48 (42,840 seconds of the simulation time), the transient reaction can be noticed.

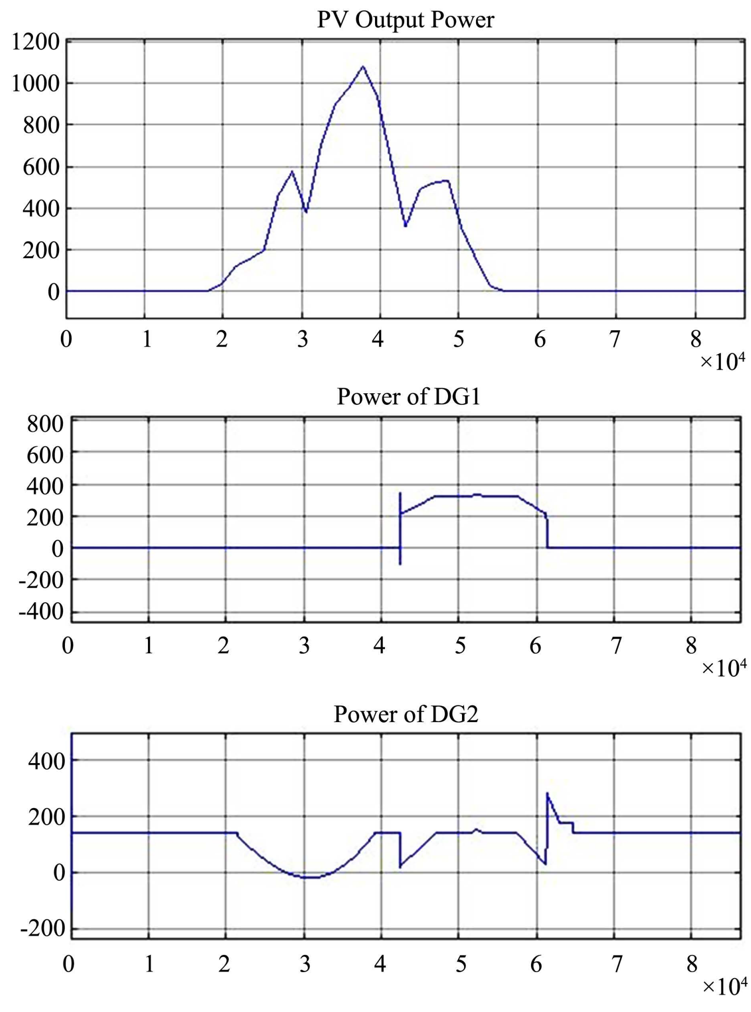

Figure 9. The output power flow at PV, DG1, and DG2.

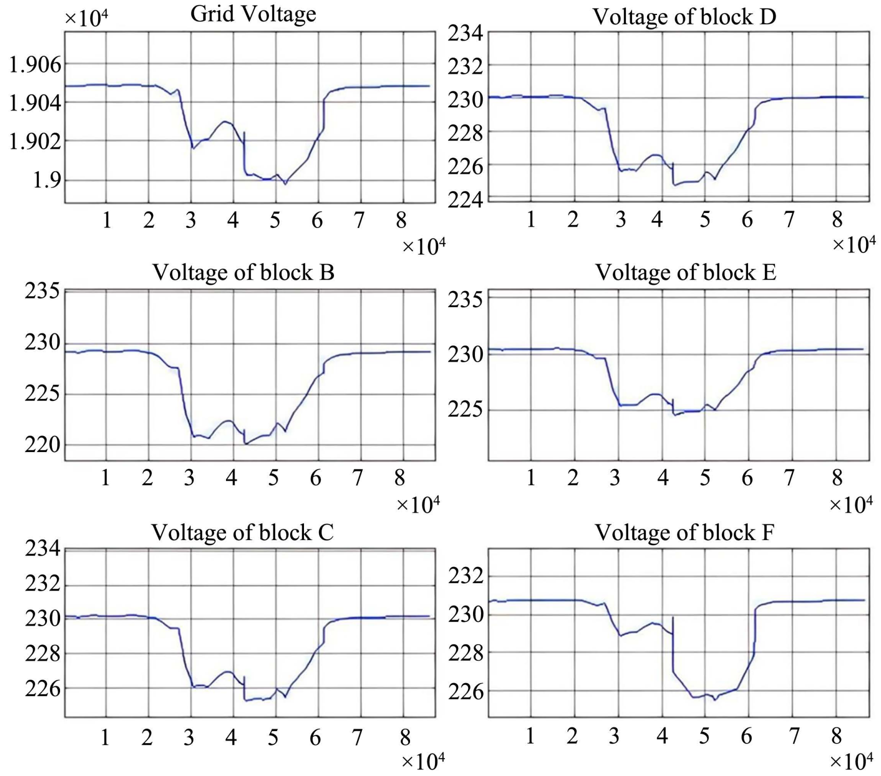

Figure 10. Voltage variations of the grid and buildings B – F.

Figure 10 shows voltage variations of the Grid and voltage readings at Buildings B – F. The grid voltage variations remain between 0.00019 - 0.0001906, and the voltage variations at different buildings stay between 220 - 231 V, indicating a completely stable microgrid. Distribution companies generally permit voltage variation within ±10% of the declared voltage based on the IEC (International Electric Code). More significant voltage variations may lead to a complete blackout and may result in damage to connected devices.

7. Conclusions

This paper presents the optimal scheduling of MG with no storage. The objective is to showcase GJU MG as a feasible, resilient, cost-effective islanded MG operation with PV and DG generation resources. The MG is an AC mid-size with a 1.8 MW PV installed capacity. The high operational cost of MG is driven by DG and the utility grid, formally defined as a non-linear convex optimization problem. We used the interior point method to solve for the optimal schedules of DG for scenario A when grid energy prices remain constant and scenario B when the prices vary. The results of optimal schedules in scenario A show daily cost savings of $1 k with a complete islanded MG operation compared to a grid-connected MG. On the other hand, the results of optimal schedules in scenario B (hypothetical) show daily cost savings of $75 compared to a grid-connected MG. The simulation results for both scenarios also show an acceptable range of voltage variations due to the availability of capacitor banks at MG.

In conclusion, we provide implications for MGs that operate in a similar setup as GJU and in the same environmental zone where the sun shines for about 300 days a year. The implications are:

- MG can be optimally and safely operated with no battery storage requirements if there exists enough DG generation capacity
- MG can be cost-effective and resilient if operated in an islanded mode and can provide large amounts of cost savings if enough PV installed capacity exists.
- MG can be guaranteed to operate in the 70% - 100% local power availability level range if there exists sufficient local generation potential of PV and DG.
- MG's high availability levels of local power can potentially reduce operational costs in return for investment and contribute to clean energy.

Future research will investigate primary and secondary control of MG operational scenarios using agents. Providing a complete agent-based MG operational control remains a challenging research problem.

Acknowledgements

This work has been partially supported by the EC FP7 ERANETMED project named "3DMicroGrid" with project number: ERANETMED_ENERG—11—286.

Conflicts of Interest

The authors declare no conflicts of interest regarding the publication of this paper.

References

[1] Madni, A.M. and Jackson, S. (2009) Towards a Conceptual Framework for Resilience Engineering. *IEEE Systems Journal*, **3**, 181-191. https://doi.org/10.1109/JSYST.2009.2017397

[2] Gholami, A., Aminifar, F. and Shahidehpour, M. (2016) Front Lines against the Darkness: Enhancing the Resilience of the Electricity Grid through Microgrid Facilities. *IEEE Electrification Magazine*, **4**, 18-24. https://doi.org/10.1109/MELE.2015.2509879

[3] Che, L., Khodayar, M. and Shahidehpour, M. (2014) Only Connect: Microgrids for Distribution System Restoration. *IEEE Power and Energy Magazine*, **12**, 70-81. https://doi.org/10.1109/MPE.2013.2286317

[4] Gholami, A., Shekari, T. and Grijalva, S. (2017) Proactive Management of Microgrids for Resiliency Enhancement: An Adaptive Robust Approach. *IEEE Transactions on Sustainable Energy*, **10**, 470-480. https://doi.org/10.1109/TSTE.2017.2740433

[5] Stluka, P. Godbole, D. and Samad, T. (2011) Energy Management for Buildings and Microgrids. 2011 50*th IEEE Conference on Decision and Control and European Control Conference*, Orlando, 12-15 December 2011, 5150-5157. https://doi.org/10.1109/CDC.2011.6161051

[6] Eajal, A.A., El-Saadany, E.F., Elrayani, Y. and Ponnambalam, K. (2014) Two-Stage Stochastic Power Generation Scheduling in Microgrids. 2014 *IEEE 27th Canadian Conference on Electrical and Computer Engineering*, Toronto, 4-7 May 2014, 1-6. https://doi.org/10.1109/CCECE.2014.6901021

[7] Gazijahani, F.S., Hosseinzadeh, H., Abadi, A. and Salehi, J. (2017) Optimal Day Ahead Power Scheduling of Microgrids Considering Demand and Generation Uncertainties. 2017 *Iranian Conference on Electrical Engineering*, Tehran, 2-4 May 2017, 943-948. https://doi.org/10.1109/IranianCEE.2017.7985174

[8] Abdolrasol, M.G.M., Hannan, M.A., Mohamed, A., Amiruldin, U.A.U., Abidin, I.B.Z. and Uddin, M.N. (2018) An Optimal Scheduling Controller for Virtual Power Plant and Microgrid Integration Using the Binary Backtracking Search Algorithm. *IEEE Transactions on Industry Applications*, **54**, 2834-2844. https://doi.org/10.1109/TIA.2018.2797121

[9] Liu, Y., Meng, T., Liu, J. and Qu, Z. (2017) Independent Microgrid Day-Ahead Optimization Based on Demand Response. 2017 29*th Chinese Control and Decision Conference*, Chongqing, 28-30 May 2017, 5809-5814. https://doi.org/10.1109/CCDC.2017.7978205

[10] Chen, J.J., Qi, B.X., Rong, Z.K., Peng, K., Zhao, Y.L. and Zhang, X.H. (2021) Multi-Energy Coordinated Microgrid Scheduling with Integrated Demand Response for Flexibility Improvement. *Energy*, **217**, Article ID: 119387. https://doi.org/10.1016/j.energy.2020.119387

[11] Moghaddam, M.M., Marzband, M. and Parhizi, N. (2016) Optimal Energy Scheduling for a Grid-Connected Microgrid Based on Multi-Period Imperialist Competition Algorithm. 2016 *IEEE International Conference on Power and Energy*, Melaka, 28-29 November 2016, 44-49. https://doi.org/10.1109/PECON.2016.7951470

[12] Luna, A.C., Diaz, N.L., Savaghebi, M., Feng, W., Sun, K., Vasquez, J. and Guerrero, J. (2017) Generation and Demand Scheduling for a Grid-Connected Hybrid Microgrid Considering Price-Based Incentives. *IECON* 2017—43*rd Annual Conference of the IEEE Industrial Electronics Society*, Beijing, 29 October-1 November 2017, 2498-2503. https://doi.org/10.1109/IECON.2017.8216420

[13] Hasankhani, A. and Hakimi, S.M. (2021) Stochastic Energy Management of Smart Microgrid with Intermittent Renewable Energy Resources in Electricity Market. *Energy*, **219**, Article ID: 119668. https://doi.org/10.1016/j.energy.2020.119668

[14] Vahedipour-Dahraie, M., Najafi, H., Anvari-Moghaddam, A. and Guerrero, J.M. (2018) Optimal Scheduling of Distributed Energy Resources and Responsive Loads in Islanded Microgrids Considering Voltage and Frequency Security Constraints. *Journal of Renewable and Sustainable Energy*, **10**, Article ID: 025903. https://doi.org/10.1063/1.5027416

[15] Kim, R.-K., Glick, M.B., Olson, K.R. and Kim, Y.-S. (2020) MILP-PSO Combined Optimization Algorithm for an Islanded Microgrid Scheduling with Detailed Battery ESS Efficiency Model and Policy Considerations. *Energies*, **13**, Article No. 1898. https://doi.org/10.3390/en13081898

[16] Chen, S.X., Gooi, H.B. and Wang, M.Q. (2012) Sizing of Energy Storage for Microgrids. *IEEE Transactions on Smart Grid*, **3**, 142-151. https://doi.org/10.1109/TSG.2011.2160745

[17] Stluka, P., Godbole, D. and Samad, T. (2011) Energy Management for Buildings and Microgrids. 2011 50*th IEEE Conference on Decision and Control and European Control Conference*, Orlando, 12-15 December 2011, 5150-5157. https://doi.org/10.1109/CDC.2011.6161051

[18] Koltsaklis, N.E., Giannakakis, M. and Georgiadis, M.C. (2018) Optimal Energy Planning and Scheduling of Microgrids. *Chemical Engineering Research and Design*, **131**, 318-332. https://doi.org/10.1016/j.cherd.2017.07.030

[19] Bolurian, A., Akbari, H. and Mousavi, S. (2022) Day-Ahead Optimal Scheduling of

Microgrid with Considering Demand Side Management under Uncertainty. *Electric Power Systems Research*, **209**, Article ID: 107965.
https://doi.org/10.1016/j.epsr.2022.107965

[20] Carpinelli, G., Mottola, F., Proto, D. and Russo, A. (2017) A Multi-Objective Approach for Microgrid Scheduling. *IEEE Transactions on Smart Grid*, **8**, 2109-2118.
https://doi.org/10.1109/TSG.2016.2516256

[21] Zhong, J. and Wang, Y. (2022) Optimal Scheduling in Rural Community Microgrids. 2022 *IEEE PES Innovative Smart Grid Technologies-Asia* (*ISGT Asia*), Singapore, Singapore, 1-5 November 2022, 225-229.
https://doi.org/10.1109/ISGTAsia54193.2022.10003557

[22] Wright, M.H. (2004) The Interior-Point Revolution in Optimization: History, Recent Developments, and Lasting Consequences. *Bulletin of the American Mathematical Society*, **42**, 39-56. https://doi.org/10.1090/S0273-0979-04-01040-7

[23] APMonitor Optimization Suite. Apmonitor.com. http://apmonitor.com/

[24] The 3DMicrogrid Project [2017-2020]. https://www.3dmicrogrid.com/home.html

[25] Al-Agtash, S., Al-Mutlaq, N., Elabbas, M., Alkhraibat, A. and Al Hashem, M. (2021) Multi-Agents for Microgrids. *Energy and Power Engineering*, **13**, 293-305.
https://doi.org/10.4236/epe.2021.137020

[26] Al-Agtash, S., Alkhraibat, A., Al Hashem, M. and Al-Mutlaq, N. (2021) Real-Time Operation of Microgrids. *Energy and Power Engineering*, **13**, 51-66.
https://doi.org/10.4236/epe.2021.131004

[27] Bintoudi, A.D., Zyglakis, L., Tsolakis, A.C., Ioannidis, D., Hadjidemetriou, L., Zacharia, L., Al-Mutlaq, N., Al-Hashem, M., Al-Agtash, S., Kyriakides, E., Demoulias, C. and Tzovaras, D. (2020) Hybrid Multi-Agent-Based Adaptive Control Scheme for AC Microgrids with Increased Fault-Tolerance Needs. *IET Renewable Power Generation*, **14**, 13-26. https://doi.org/10.1049/iet-rpg.2019.0468